PALEOCEANOGRAPHY, VOL. 27, PA3205, doi:10.1029/2011PA002249, 2012

A multiproxy record of terrestrial inputs to the coastal ocean using minor and trace elements (Ba/Ca, Mn/Ca, Y/Ca) and carbon isotopes (δ^{13}C, Δ^{14}C) in a nearshore coral from Puerto Rico

Ryan P. Moyer,[1] Andréa G. Grottoli,[1] and John W. Olesik[1]

Received 13 October 2011; revised 8 March 2012; accepted 11 June 2012; published 19 July 2012.

[1] Small mountainous rivers (SMRs), despite their disproportionate size relative to larger rivers, may contribute as much as one third of the total terrigenous material exported to the coastal ocean. Corals growing near the mouths of tropical SMRs have the potential to provide records of terrigenous material fluxes because they are long lived and elemental and isotope signatures within their skeletons are useful proxies of palaeoceanographic variability. Here, a 56 year record of coral skeletal Ba/Ca, Mn/Ca, Y/Ca, δ^{13}C, and Δ^{14}C measurements is presented from a *Montastraea faveolata* colony growing ~1 km from the mouth of an SMR in eastern Puerto Rico. Coral Ba/Ca was coherent with river discharge and coral skeletal δ^{13}C at annual periodicity corresponding to synchronous depletions of both δ^{13}C and Δ^{14}C in the coral skeleton, and Mn/Ca and Y/Ca were not coherent with river discharge at annual periodicity. Coherence between river discharge and Ba/Ca and the concurrent timing of increases in Ba/Ca with decreases in δ^{13}C and Δ^{14}C indicate that river discharge is simultaneously recorded by all three geochemical tracers. A reconstruction of Rio Fajardo discharge is presented for a period in which no instrumental discharge records exists shows good fidelity with the timing of increased discharge during the wet season. Thus, coral-based multiple-proxy records can be valuable tools for reconstructing the timing and variability of SMR discharge to the coastal ocean. Such records are critical to understanding changes in material fluxes and biogeochemical cycles in coastal environments due to land use and climate change.

Citation: Moyer, R. P., A. G. Grottoli, and J. W. Olesik (2012), A multiproxy record of terrestrial inputs to the coastal ocean using minor and trace elements (Ba/Ca, Mn/Ca, Y/Ca) and carbon isotopes (δ^{13}C, Δ^{14}C) in a nearshore coral from Puerto Rico, *Paleoceanography*, *27*, PA3205, doi:10.1029/2011PA002249.

1. Introduction

[2] Rivers are principal sources of terrestrial sediments, minor and trace elements, and organic material to coastal waters. Small mountainous rivers (SMRs) are thought to be major sources of terrestrial material to the world's oceans [e.g., *Milliman and Syvitski*, 1992], and tropical SMRs may contribute as much as one third of the terrigenous material exported to the global coastal oceans [e.g., *Lyons et al.*, 2002]. The ability to quantify terrigenous inputs to the coastal ocean and understand how they have changed through time is critical to understanding local and global elemental budgets (including carbon) in the context of modern anthropogenic land use and climate changes. However, few instrumental data are available for the majority of SMRs in the topical Atlantic or Indo-Pacific regions, thus representing a major gap in our understanding of global biogeochemical cycles. Minor and trace elements in coral skeletons [e.g., *Alibert et al.*, 2003; *McCulloch et al.*, 2003; *Sinclair and McCulloch*, 2004; *Fleitmann et al.*, 2007; *Lewis et al.*, 2007] and foraminfera [e.g., *Weldeab et al.*, 2007a, 2007b] have been shown to be effective recorders of terrestrial inputs to the coastal ocean for large, continental rivers. Recent work has also shown that isotope records from corals growing near SMRs can provide a history of terrestrial carbon input to the coastal ocean [*Moyer and Grottoli*, 2011]. However, coral-based elemental records from SMRs have not been previously reported in the literature, and such records may serve as useful proxies of terrestrial elemental fluxes in the tropics, where instrumental records are often scarce.

[3] Corals are long lived (300+ years), occur in nearly all shallow tropical waters, and elemental and isotopic variations within their skeletons serve as useful proxy records of palaeoceanographic variability (see reviews by *Shen and Sanford* [1990], *Druffel* [1997], *Gagan et al.* [2000], *Mark*

---

[1] School of Earth Sciences, Ohio State University, Columbus, Ohio, USA.

Corresponding author: R. P. Moyer, School of Earth Sciences, Ohio State University, 125 South Oval Mall, Columbus, OH 43201, USA. (ryan.p.moyer@gmail.com)

0883-8305/12/2011PA002249

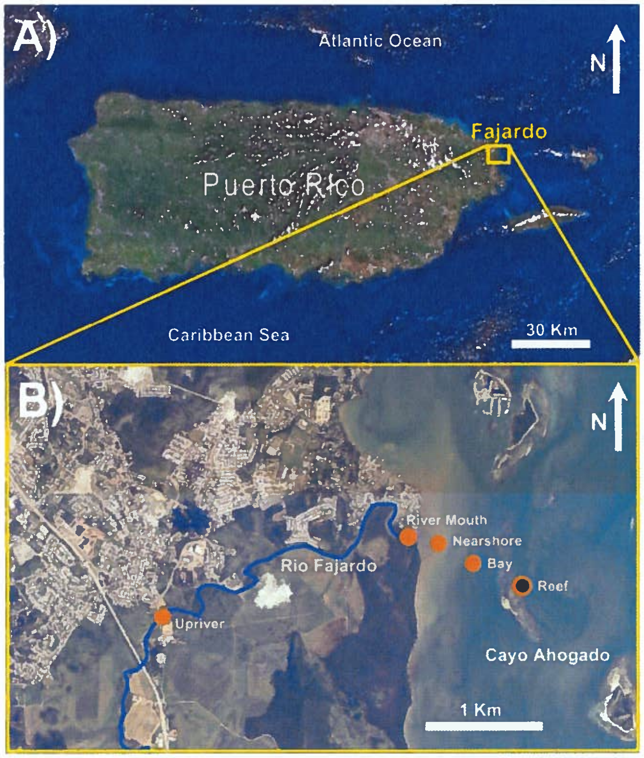

Figure 1. Study area. (a) Landsat 7 image of Puerto Rico, showing the location of the Fajardo study area within Puerto Rico. (b) USGS 1:24,000 aerial image mosaic of the lower Rio Fajardo catchment. Orange circles indicate trace element sampling sites, and the black circle with the orange ring indicates where the Fajardo coral core was collected as well as the water sampling location over the reef at Cayo Ahogado. Landsat 7 source: www.nasa.gov; aerial image source: www.usgs.gov.

Eakin and Grottoli [2006], and *Grottoli and Mark Eakin* [2007]). Paired stable ($\delta^{13}C$) and radiocarbon ($\Delta^{14}C$) isotope measurements in coral skeleton have been shown to reflect the input of riverine dissolved inorganic carbon (DIC) to the coastal ocean [*Moyer and Grottoli*, 2011]. Additionally, trace element concentrations in corals growing in nearshore environments have been shown to record natural and anthropogenically induced changes in the delivery of terrigenous material to the coastal ocean [*McCulloch et al.*, 2003; *Sinclair and McCulloch*, 2004; *Fleitmann et al.*, 2007; *Lewis et al.*, 2007]. The development of laser ablation inductively coupled plasma mass spectrometry (LA-ICP-MS) measurement techniques specific to coral skeletons [see *Sinclair et al.*, 1998; *Fallon et al.*, 1999; *Matthews*, 2007] has created the ability to produce high-resolution minor and trace element records over long periods of time.

[4] Of the numerous minor and trace elements that have previously been measured in corals, barium (Ba), manganese (Mn), and yttrium (Y) have been shown to have the closest association with river discharge and terrestrial inputs [e.g., *Shen and Sanford*, 1990; *Swart et al.*, 1999; *Alibert et al.*, 2003; *McCulloch et al.*, 2003; *Sinclair and McCulloch*, 2004; *Wyndham et al.*, 2004; *Fleitmann et al.*, 2007; *Lewis et al.*, 2007; *Prouty et al.*, 2008; *Carilli et al.*, 2009; *Prouty et al.*, 2010]. Ba becomes a tracer of terrigenous sediment in the ocean after desorbing from fine-grained sediments in low-salinity estuarine environments, and then mixing conservatively along the freshwater-seawater salinity gradient [*Edmond et al.*, 1978; *Li and Chan*, 1979]. Once in the marine environment, Ba can substitute for Ca in the coral skeleton in proportion to its concentration in seawater [*Lea et al.*, 1989]. Additional studies have suggested that Ba can also be incorporated into the coral skeletal matrix along with fine sediment particles, which are also commonly rich in Ba [*Sinclair and McCulloch*, 2004]. Similar to Ba, Mn and Y also exhibit desorption from suspended particulate matter in low-salinity waters and can become incorporated in coral skeletons. At annual resolution (or longer), Mn/Ca and Y/Ca in corals are effective tracers of anthropogenic activities on land [e.g., *Fallon et al.*, 2002; *Lewis et al.*, 2007; *Prouty et al.*, 2008; *Carilli et al.*, 2009]. However, at subannual resolution both Mn and Y appear to be less sensitive to riverine inputs than Ba [*Lewis et al.*, 2007; *Prouty et al.*, 2009].

[5] Since minor and trace elements and carbon isotopes in corals all record terrestrial geochemical influence in the coastal ocean, a combined multiple-proxy approach using minor and trace elements and carbon isotopes [*Moyer and Grottoli*, 2011] may reveal important information about terrestrial elemental fluxes to the coastal ocean. Furthermore, the use of such a multiproxy approach is also likely to enhance the information that can be gleaned from using any one tracer alone. Specifically, coral skeletal minor and trace element ratios combined with $\delta^{13}C$ and $\Delta^{14}C$ measurements may provide a clearer record of riverine solute fluxes to the coastal ocean than any single proxy alone. Thus, the goal of this study was to examine the relationship of coral Ba/Ca, Mn/Ca, and Y/Ca to river discharge and skeletal carbon isotopic composition ($\delta^{13}C$ and $\Delta^{14}C$) in a coral growing near the mouth of a tropical SMR. Using this multiproxy approach, the following hypotheses were addressed: 1) Ba/Ca, Mn/Ca, and Y/Ca ratios in a coral skeleton collected near the river mouth are coherent on annual time scales with river discharge, 2) coral Ba/Ca, Mn/Ca, and Y/Ca are inversely coherent with coral $\delta^{13}C$ on annual time scales, and 3) the timing of increases in coral minor and trace element ratios should cooccur with synchronous depletions of $\delta^{13}C$ and $\Delta^{14}C$ in the coral skeleton. A reconstruction of discharge using these multiple proxies is presented for an SMR in Puerto Rico. The combined use of minor and trace elements sensitive to river discharge and carbon isotopes may enable the development of quantitative proxies for the delivery of terrestrial material, including carbon, to the coastal ocean. Such information would be invaluable in the tropics where most small rivers are not gauged or regularly monitored and local inputs of solutes and sediments is not well understood. These data are critical to understanding how past, present, and future land use and climate change can impact the delivery of terrestrial material and alter associated nearshore biogeochemical cycles on local to global scales.

2. Materials and Methods

2.1. Study Area

[6] The Rio Fajardo drains a small catchment area of about 70 km^2 in northeastern Puerto Rico (Figure 1). Annual rainfall within the Fajardo catchment is spatially variable,

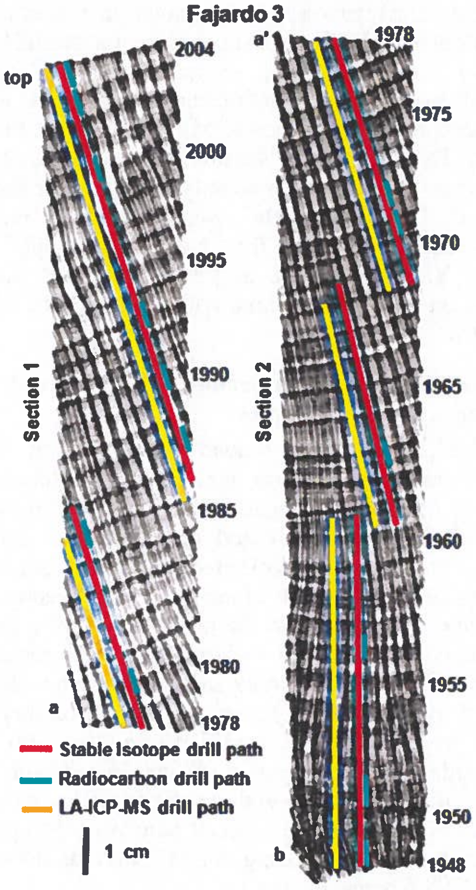

Figure 2. X-radiograph positive prints of the Fajardo coral core. The drill paths for stable (red lines) and radiocarbon (light blue lines) isotopic analyses and the laser ablation inductively coupled plasma mass spectrometry (LA-ICP-MS) scan paths for trace element measurement (yellow lines) are shown. The age model based on annual bands is indicated along the right side of each core section.

with the mountainous headwaters receiving up to 4500 mm yr^{-1}, while the coastal plain receives about 1,500 mm yr^{-1} [*Clark and Wilcock*, 2000]. Peak rainfall generally occurs during the months of May, October, and November and peak river discharge occurring during the months of October and November. The main river within the catchment, the Rio Fajardo, is fed by several smaller streams originating in the Luquillo Mountains and flows seaward in a general east-west direction. At its headwaters, the Rio Fajardo drains a tropical rain forest with steep volcanic bedrock valleys, while the downstream portion of the river drains recent alluvium to the head of the coastal plain. The town of Fajardo is situated along the north banks of the Rio Fajardo near the river mouth where flow becomes tidally influenced (tidal range <1 m) [*Clark and Wilcock*, 2000]. The Rio Fajardo discharges into Vieques Sound, a large, shallow, semienclosed basin in eastern Puerto Rico. A small coral reef, Cayo Ahogado, is located approximately 1 km from the mouth of the Rio Fajardo (Figure 1b). This reef is characterized by low percent cover of scleractinian and alcyonacean corals [*Goenaga and Cintron*, 1979], with members of the genera *Montastraea*, *Porites*, and *Siderastrea* being the most common scleractinian coral species.

[7] Puerto Rico has seen major shifts in land use within the last 200 years. Prior to the 1800s the landscape was largely forested with a total land cover of 3% cropland, 24% pasture, and 73% remaining forested [*Gellis*, 2003]. By 1899, agriculture became the dominant economic driver in Puerto Rico, resulting in significant land use change. At this time, pasture covered 55% of island [*Grau et al.*, 2003], agricultural cropland accounted for 21% [*Gellis*, 2003], and only 24% of the natural vegetation remained. The use of land for agriculture peaked in 1939 when 85% of the landscape was pasture or cropland [*Grau et al.*, 2003], and by 1948 forest cover in Puerto Rico decreased to 6.5% of the total land area [*Gellis*, 2003]. A major economic shift away from agriculture and toward industry and tourism occurred between 1950 and 1980, and resulted in a corresponding change in land use. Between the 1940s and the 1990s, agricultural land cover decreased from 85% to 37% [*Grau et al.*, 2003], and during the period 1977–1994 urban land cover increased by 27.4% [*López et al.*, 2001]. The history of land use change in the Fajardo catchment is typical of Puerto Rico, and partial reforestation due to agricultural abandonment has occurred within the catchment. Present land cover within the Fajardo catchment consists of ~46% partly developed or abandoned lands [*Lugo and Helmer*, 2004], 30% active cropland and pasture, 8% coniferous forest, 7% lowland forest, 4.0% developed land, and 4% grassland [*Hearn et al.*, 2001].

2.2. Coral Sampling

[8] On 5 October 2004, a 3 cm diameter core (Core ID: FJ3, referred to as the Fajardo coral throughout) was taken from a *Montastraea faveolata* coral colony growing on the seaward fore reef slope of Cayo Ahogado (N 18° 19.413′; W 065° 37.084′) at 4 m depth using a handheld submersible pneumatic drill. The colony selected for coring was alive and had no visible signs of partial or mass mortality at the top of the colony where the core was taken, and did not appear to be undercut by bioerosion at the base of the colony. A total of four core segments with a total length of 62.5 cm were extracted from the coral along the maximum axis of upward growth. Each core segment was longitudinally slabbed, cleaned, and X-radiographed in order to determine the growth chronology of the coral colony by examining the annual density bands within the coral skeleton [*Knutson et al.*, 1972; *Buddemeier and Kinzie*, 1976]. X-radiographs of the top two sections of the Fajardo core revealed the presence of 56 distinct annual density bands spanning the period from 1948 to 2004 (Figure 2). X-radiographs of the remaining two core sections revealed that the growth bands in those sections were not oriented along the major growth axis, and were therefore not used for further analyses. Annual linear skeletal extension (LSE) ranged from 3.8 to 8.1 mm yr^{-1} with a mean annual LSE rate of 5.72 ± 1.20 mm yr^{-1}. Detailed methods for preparation, X-radiography, and establishment of the growth chronology of the Fajardo core are given by *Moyer and Grottoli* [2011].

2.3. Coral Minor and Trace Element Analyses

[9] After removal of material for stable isotope analysis, the Fajardo coral slabs were sectioned into seven 25 ×

45 mm pieces for analysis via laser ablation inductively coupled plasma mass spectrometry (LA-ICP-MS) in the Trace Element Research Laboratory at the Ohio State University. Prior to analysis, each section was individually cleaned for 30 min in a high-intensity ultrasonic bath using 18 mΩ Milli-Q® water and dried overnight in an oven at 60°C. Core slices were then mounted into an ablation cell with a motorized stage and scanned beneath a 193 nm ArF excimer laser with beam homogenizing optics (New Wave UP-193-HE). Scan paths were selected to be parallel to both the major growth axis of the coral, as well as to the stable isotope sampling drill path (Figure 2). At the sample surface, the laser beam was 40×385 μm with the long axis oriented perpendicular to the growth axis of the coral. The laser was pulsed at 10 Hz and between 12 and 15 J cm^{-2}. Ablated material was carried to the plasma of a Thermo- Finnigan Element 2 ICP-Sector Field MS (ICP-SFMS) with fast magnet scan and high abundant sensitivity options via a continuous 0.8 L min^{-1} He stream that was mixed with 1.0 L min^{-1} Ar after the ablation cell. Measurements were preceded by ~10 s of background acquisitions. Each section was scanned at a rate of approximately 20 μm/s, with spectra being collected every 0.4 –0.7 s.

[10] The isotopes ^{25}Mg, ^{43}Ca, ^{55}Mn, ^{86}Sr, ^{89}Y, and ^{138}Ba were measured with ^{43}Ca being used as an internal standard to correct for signal fluctuations brought about by surface irregularity and changes in skeletal density of the coral skeleton. The ICP-SFMS was operated in medium mass spectral resolution (R = 5000) in order to completely resolve the small $^{89}Y^{+}$ signal from the tail of the very large $^{88}Sr^{+}$ signal. Autolock mass was used to minimize mass drift. Measured signal values of the isotopes ^{55}Mn, ^{89}Y, and ^{138}Ba were normalized to the measured ^{43}Ca of the sample to give concentrations relative to the aragonite [*Fallon et al.*, 1999]. Each section of the Fajardo core was scanned a total of six times along the same sampling path. The first three scans were treated as cleaning scans similar to methods reported for other recent measurements of minor and trace elements in coral skeletons [e.g., *Fallon et al.*, 1999; *Alibert et al.*, 2003; *Sinclair and McCulloch*, 2004; *Sinclair*, 2005; *Lewis et al.*, 2007; *Fleitmann et al.*, 2007]. The concentrations of each element measured during scans four through six were highly reproducible (average relative standard deviation = 6%) and data from these scans were used for data analysis. See section 2.6 for additional details.

[11] Measurements of instrument background and known standards were collected before and after the analysis of the coral sections in order to correct for any long-term instrument drift. Synthetic glass standard reference materials (SRMs) were determined to be the most suitable for minor and trace element quantification in corals [e.g., *Craig et al.*, 2000; *Fallon et al.*, 2002; *Matthews*, 2007]. Two glass SRMs (NIST 610 and NIST 612) were mounted in the ablation cell along with the coral section and each were scanned prior to, and following, the scans made on each coral section. A separate experiment was performed to establish accuracy of the measurements, and test for matrix effects between glass (NIST 610 and 612) and calcium carbonate materials using a multielement carbonate standard (USGS MACS-1). The ratio of the M/Ca signals to reported M/Ca concentrations in the glass standards were within 10% for Mn and Ba when compared to MACS-1. Thus, under the analytical parameters used in this study, matrix effects were small. Published Y concentrations were not available for the MACS-1 at the time of this study. The NIST 610 and 612 standards were measured before and after each line scan, and typical relative standard deviations (RSDs) were between 1 and 5%. Drift in relative sensitivities was typically below 10%. Signal to blank ratios were typically higher than 100:1 for $^{43}Ca^{+}$, $^{86}Sr^{+}$ and $^{138}Ba^{+}$. Signal to blank ratios were typically higher than 50:1 for $^{25}Mg^{+}$, $^{55}Mn^{+}$, and $^{89}Y^{+}$. All reported Y/Ca values are at least 1 order of magnitude greater than the detection limit, which was about 0.003 μmol Y/mol Ca.

2.4. Sampling and Measurement of Minor and Trace Elements in Ambient Waters

[12] Ambient river and seawater samples were collected for minor and trace element analysis along a transect from upriver to the Cayo Ahogado reef (Figure 1b) on 19 March 2008. Samples were collected by hand from subsurface waters (10 to 20 cm) in precleaned low-density polyethylene bottles (LDPE) at each site along the transect. Samples were stored cold (~4°C) and in the dark while in the field, and then filtered and acidified within 4 days upon return to the laboratory. Throughout, water samples were handled using Nitrile™ polyethylene gloves. In the laboratory, water samples were filtered and acidified in a Class 100 laminar flow hood. Filtration towers were precleaned with 18 mΩ Milli-Q® water and fitted with Nucleopore™ polycarbonate membrane filters (0.4 μm nominal pore size). Samples were acidified to 2% (v/v) using VERITAS® double-distilled HNO_3 (GFS Chemicals, Inc.).

[13] Low-salinity (<5) water samples were measured undiluted using a PerkinElmer Sciex ELAN 6000 ICP-MS. External standard solutions with known concentrations of dissolved Ba, Mn, and Y were used for calibration. An independent check standard was measured after every three samples to allow for correction of instrumental drift and calculation of precision. Ca and Mn signals were normalized to the signal from Sc that was added at 10 ppb as an internal standard. The Y and Ba signals were normalized to the signal from Indium (In) that was added at 10 ppb as an internal standard.

[14] Samples having salinities greater than 5 were diluted by a factor of ten and the concentrations of Ca, Ba, Mn, and Y were measured using a Thermo-Finnigan Element 2 ICP-SFMS. A duplicate Fajardo Reef sample spiked with two different concentrations of Ba, Mn, Y and Ca was used as a standard for addition calibration [*Thomas*, 2003] of the measurements. Mn^{+}, Y^{+} and Ba^{+} were measured in low-resolution mode (R = 400). Sc (1 ppb) was used as an internal standard for Mn, and In (1 ppb) was used as an internal standard for Y and Ba. Ca^{+} was measured in medium resolution mode (R = 4000) and normalized to the internal In standard signal. Average RSDs derived from repeated measurements of three check standards used to correct for instrumental drift were 4%, and never exceeded 10%.

2.5. Isotopic Analyses

[15] Detailed methods on the isotopic analysis of the Fajardo core are given by *Moyer and Grottoli* [2011]. Briefly, coral skeleton for stable isotope analysis was shaved

at 1 mm intervals (n = 232) along a path parallel to the axis of growth in the top two sections of the Fajardo core (Figure 2). Additional skeletal material for radiocarbon analysis (n = 54) was drilled in a horizontal plane immediately adjacent to the stable isotope path at targeted intervals (Figure 2). Coral $\delta^{13}C$ was measured with a Finnigan MAT 252 triple collecting stable isotope ratio mass spectrometer (SIR-MS) in Grottoli's lab. The standard deviation of repeated measurement of NBS 19 (n = 83) and duplicate samples (n = 40) was $\leq \pm 0.05$ ‰ for $\delta^{13}C$. All coral $\delta^{13}C$ measurements are reported in per mil (‰) relative to the Vienna Pee Dee Belemnite (VPDB) standard using the conventions of *Coplen* [1996]. High-precision coral skeletal radiocarbon measurements were made using an NEC 0.5 MV compact accelerator mass spectrometer (AMS) at the Keck AMS facility at the University of California, Irvine. The standard deviation of all $\Delta^{14}C$ measurements was ±1.7 ‰. Radiocarbon measurements were reported as fraction modern and converted to $\Delta^{14}C$ (the per mil deviation of $^{14}C/^{12}C$ in the sample relative to that of the 95% Oxalic Acid-1 standard) according to the conventions of *Stuiver and Polach* [1977].

2.6. Data Analysis

[16] LA-ICP-MS data acquired for each element during each scan were converted to an ASCII file using the Element 2 ICP-SFMS instrument software. Data for each standard and each scan were imported into a separate spreadsheet and then reduced using a ten-point moving average to reduce the impact of peak hopping during analysis. An average of the background signal obtained before each standard and sample measurement was subtracted from the signals for each standard and sample. Elemental ratios in the form of (M signal/Ca signal)/(M mmoles/Ca moles) were determined from NIST 610 and NIST 612 standards, where M is the element of interest. M/Ca concentration ratios were calculated from ten-point smoothed intensities of M and ^{43}Ca based on the "recommended" values of *Pearce et al.* [1997]. Minor and trace element measurements were then converted to time series using the growth chronology of the Fajardo coral (Figure 2) developed by *Moyer and Grottoli* [2011].

[17] The minor and trace element record of each coral section was assembled using the average of three consecutive ablation scans along the same path as described in section 2.3 above. Averaged data from each of the seven core sections was assembled in chronological order and these time series were further reduced to approximately biweekly resolution using nearest-neighbor running averages. Each minor and trace element record was then compared to river discharge data for the Rio Fajardo (USGS Station #50071000; Figure 3a) obtained from the U.S. Geological Survey (Water resources of the Caribbean, 2008, http://pr.water.usgs.gov/). Periodicity trends within individual data sets were examined using single-spectrum analysis based on a Fourier transform function, and covariation and correlation between two stochastic time series was evaluated using bivariate cross-spectral analysis [*Chatfield*, 2004]. A Hamming window (width = 5) was applied to both time series. Coherency confidence limits were estimated using the methods described by *Thompson* [1979]. Smoothed data sets were detrended by subtracting the long-term average from each value prior to analysis. Averaged values are reported as arithmetic means ± 1 standard deviation, and coherence was considered statistically significant at $p \leq 0.05$. Conservative mixing relationships of dissolved constituents (Ba, Mn, Y) between river and marine end-members were modeled by fitting a linear trend line between the freshwater and marine end-member concentrations of each element. Rio Fajardo discharge was reconstructed using multiple-regression analysis for a period where coral geochemical data exist, but no instrumental data were available. All spectral time series and multiple-regression analyses were performed using Statistica version 8 (© 2007 StatSoft, Inc.).

3. Results

3.1. Coral Minor and Trace Elements

[18] Elemental ratios of Ba/Ca, Mn/Ca, and Y/Ca in the Fajardo coral and available Rio Fajardo discharge rates are shown in Figure 3. Coral Ba/Ca ranged from 3.87 to 9.20 μmol mol^{-1}, had an overall average of 5.21 ± 0.30 μmol mol^{-1}, and increased by an average of 0.004 μmol mol^{-1} yr^{-1} over the span of the entire 56 year record (Figure 3b). Mn/Ca ratios ranged from 0.38 to 6.74 μmol mol^{-1}, averaged 1.002 ± 0.309 μmol mol^{-1}, and decreased by 0.003 μmol mol^{-1} yr^{-1} over the span of the entire record (Figure 3c). Last, Y/Ca in the Fajardo coral ranged from 1.04×10^{-3} to 0.41 μmol mol^{-1}, averaged 0.04 ± 0.02 μmol mol^{-1}, and remained constant over the span of the 56 year record (Figure 3d).

[19] Single-spectrum analysis revealed that Ba/Ca displayed annual periodicity (Figure 4a). Annual Ba/Ca peaks typically occurred in the latter half of each calendar year from August to January, and were most frequent in November. Cross-spectral analysis of Rio Fajardo discharge and the Ba/Ca time series revealed significant annual coherence (0.950) at the 99% confidence limit (Figures 4a and 4b). Rio Fajardo discharge and coral Ba/Ca covaried with a nearly in-phase relationship (phase angle = 29°) with Ba/Ca lagging river discharge. The relationship was such that as discharge increased coral Ba/Ca also increased with an average lag of 6 ± 1 weeks. Ba/Ca and $\delta^{13}C$ anomalies in the Fajardo coral were also annually coherent (0.695) at the 80% confidence limit (Figures 4c and 4d). Coral Ba/Ca and $\delta^{13}C$ anomalies covaried with a nearly antiphase relationship (phase angle = 160°) such that as Ba/Ca increased, $\delta^{13}C$ anomalies decreased. Annual peak Ba/Ca ratios lagged the occurrence of $\delta^{13}C$ minima by approximately 8 ± 1 weeks.

[20] Single-spectrum analysis revealed Mn/Ca to have 2.5 year periodicity over the entire detrended coral record. Cross-spectral analysis of Rio Fajardo discharge and the Mn/Ca time series revealed significant coherence at approximately 2 year (0.736, p = 0.05) and 4.5 year (0.879, $p < 0.01$) intervals (Figures 4e and 4f). Cross-spectral analysis of Mn/Ca and coral $\delta^{13}C$ showed no meaningful spectral relationships across all frequencies. Single- and cross-spectral analysis of Y/Ca and Rio Fajardo discharge or Y/Ca and coral $\delta^{13}C$ showed no meaningful spectral relationships across all frequencies.

3.2. Minor and Trace Elements in Natural Waters

[21] The concentration of dissolved Ba ranged from 71.5 to 273.7 nmol kg^{-1} and was lowest at the marine end-member site above the reef and highest at intermediate

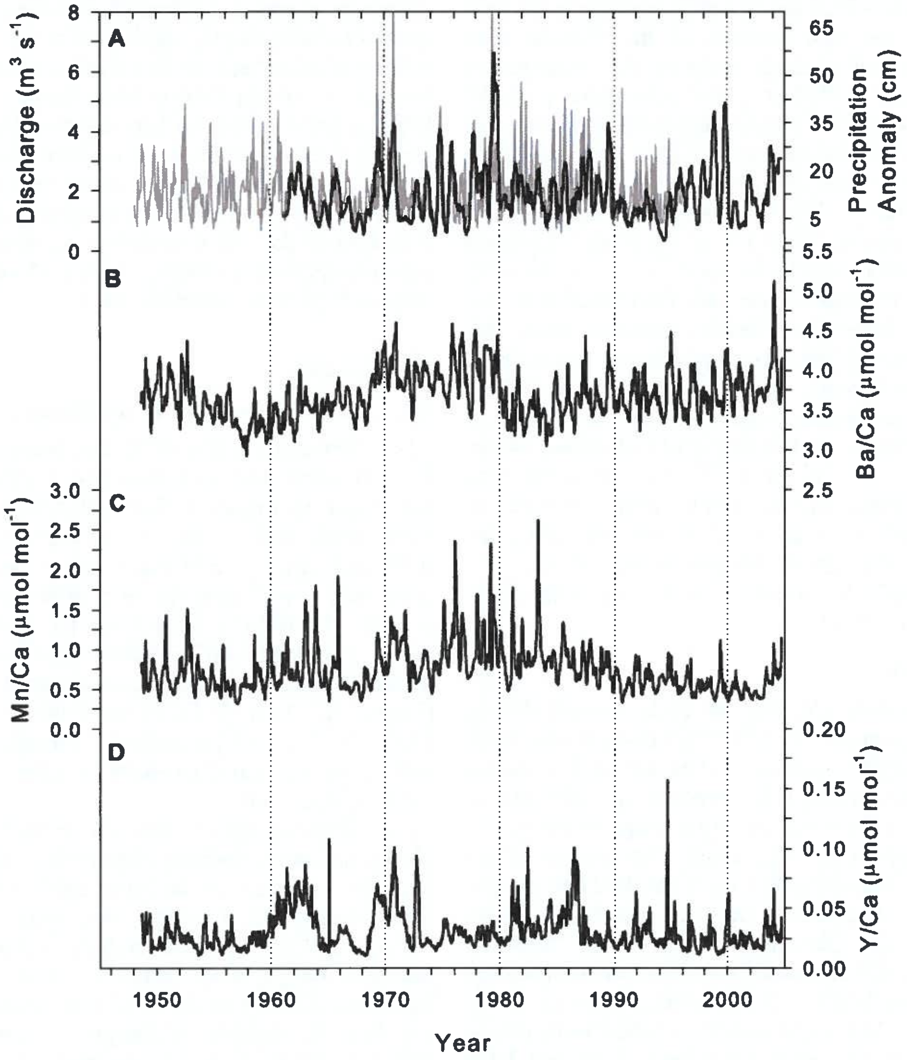

Figure 3. River discharge and coral trace element ratio time series. (a) Fajardo precipitation anomalies (gray line) and Rio Fajardo discharge (black line) and coral (b) Ba/Ca, (c) Mn/Ca, and (d) Y/Ca ratios for the period 1948–2004. All data have been smoothed to approximately biweekly resolution. Precipitation data were obtained from NOAA National Climate Data Center station #663657 (http://www.ncdc.noaa.gov). Rio Fajardo discharge data were obtained from USGS stream gauge station #50071000 (http://pr.water.usgs.gov).

salinities (Table 1 and Figure 5a). Dissolved Mn concentrations were nearly equal at freshwater and marine end-member sites but were 2.5 orders of magnitude greater at intermediate salinities (Table 1 and Figure 5b). Y ranged from 0.2 to 1.1 nmol kg^{-1} and had the lowest concentration of all elements measured at each site. As with Ba and Mn, the highest Y concentrations also occurred at sites with intermediate salinities (Table 1 and Figure 5c). Dissolved Ba, Mn, and Y all exhibited nonconservative mixing at sites with low to intermediate salinities (Figure 5). Dissolved Ca was the most abundant element measured at all sites and was lowest at the river end-member site (S = 0) and was highest at the Bay site (S = 36.1; Table 1).

3.3. Coral δ^{13}C and Δ^{14}C

[22] Detailed results of the δ^{13}C and Δ^{14}C measurements made in the Fajardo coral skeleton (Figure 6) have previously been reported by *Moyer and Grottoli* [2011]. Briefly, cross-spectral analysis of Rio Fajardo discharge and the coral δ^{13}C anomalies revealed significant ($p < 0.05$) annual coherence such that as discharge increased coral δ^{13}C anomalies decreased. Coral skeletal δ^{13}C and Δ^{14}C anomalies were positively correlated and synchronous depletions of both δ^{13}C and Δ^{14}C anomalies were present for the periods 1950 to 1960 and again from 1975 to 2004 (Figure 6). No clear relationship was shown between the coral skeletal δ^{13}C and Δ^{14}C anomalies for the period 1960 to 1975, which corresponds with the timing of the maximum increase in bomb radiocarbon within the Fajardo coral skeleton.

4. Discussion

4.1. Coral Ba/Ca

[23] Annual periodicity of Ba/Ca records in coral skeletons have been reported from a number of studies for a variety of coral species across the Caribbean and Indo-Pacific regions

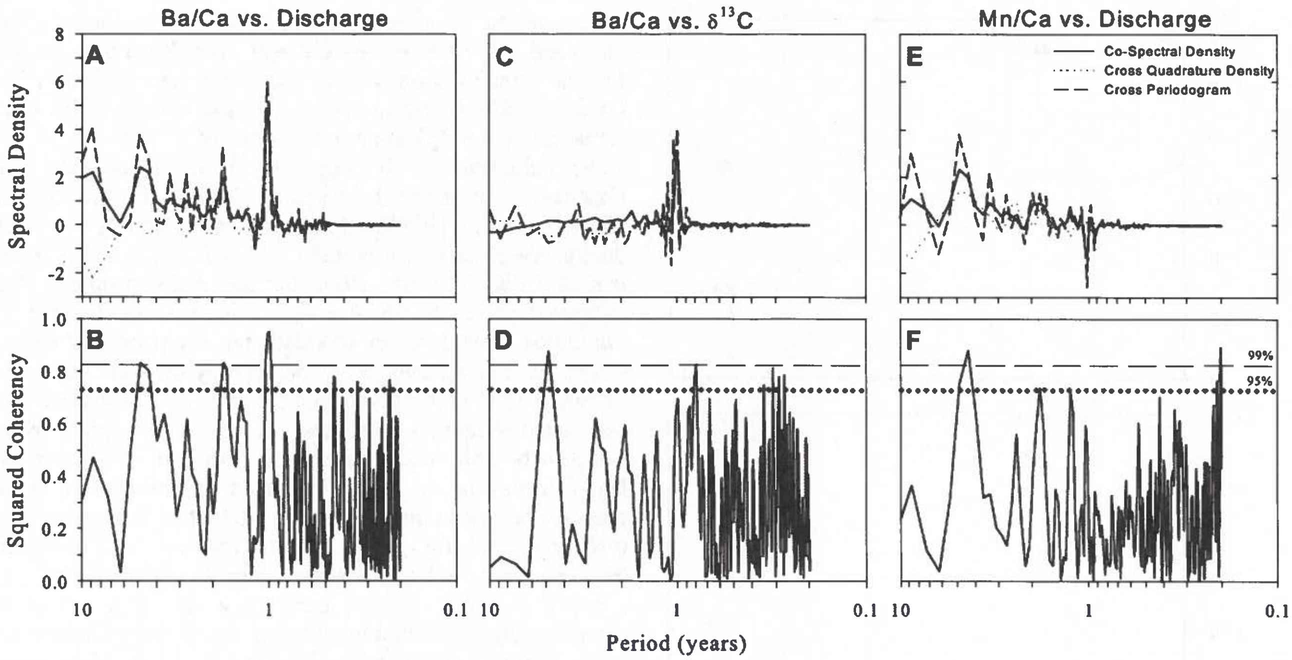

Figure 4. Results of significant cross-spectral analyses. (a) Spectral density estimates of coral Ba/Ca and Rio Fajardo discharge time series and (b) their coherence. (c) Spectral density estimates of Ba/Ca and coral $\delta^{13}C$ time series and (d) their coherence. (e) Spectral density analysis of Mn/Ca and Rio Fajardo discharge time series and (f) their coherence. Dashed lines indicate the 95% and 99% confidence limits.

[*Shen and Sanford*, 1990; *Tudhope et al.*, 1996; *Shen et al.*, 1992a; *Fallon et al.*, 1999; *Alibert et al.*, 2003; *McCulloch et al.*, 2003; *Sinclair and McCulloch*, 2004; *Wyndham et al.*, 2004]. However, the timing of annual maxima and minima can be highly variable among both location and individual records. For corals growing inshore in non-upwelling environments, the source of annual Ba/Ca variability in coral skeletons has been attributed to the seasonal wet season delivery of terrigenous Ba to the coastal ocean via rivers [*Shen and Sanford*, 1990; *Swart et al.*, 1999; *Alibert et al.*, 2003; *McCulloch et al.*, 2003; *Sinclair and McCulloch*, 2004; *Fleitmann et al.*, 2007; *Lewis et al.*, 2007]. Yet other studies have reported "anomalous" Ba records from coral skeletons in coastal waters where Ba/Ca does not reflect riverine inputs [e.g., *Hart and Cohen*, 1996; *Tudhope et al.*, 1996; *Esslemont et al.*, 2004; *Sinclair*, 2005]. In such instances, largely unspecified metabolic effects are implicated in affecting Ba/Ca records in an unpredictable way.

[24] The Fajardo coral was collected far from a shelf edge within a shallow, nonupwelling, semienclosed basin in very close proximity to the mouth of the Rio Fajardo (Figure 1). The strong coherence between Rio Fajardo discharge and coral Ba/Ca (Figures 4a and 4b) measured in this study indicate that Ba/Ca in the Fajardo coral is influenced by Ba being transported from land. Additionally, Ba/Ca maxima across the entire Fajardo coral record occur near the end of each year (Figure 3b), corresponding to the months of November through January. These occurrences coincide well with the known timing of the wet season in the Fajardo study area (May through mid-January; Figure 3a) and are lagged by one to two months relative to the timing of average peak annual river discharge (September through November; Figure 7). The lag between peak annual river discharge and peak Ba/Ca may be controlled by a number of factors including complex estuarine desorption kinetics at the river mouth [*Dorval et al.*, 2005, and references therein], wet season dilution effects [*Alibert et al.*, 2003; *Sinclair and McCulloch*, 2004] due to Ba supply limitations in tropical river catchments [*Edmond et al.*, 1978; *Sinclair and McCulloch*, 2004], or coral metabolic and growth effects [*Pingitore et al.*, 1989; *Matthews*, 2007].

[25] Estuarine processes influencing the concentration of dissolved Ba are known to be complex and coastal

Table 1. Trace Element Measurements in the Natural Waters of Fajardo, Puerto Rico[a]

Location	Salinity	Ba (nmol Kg^{-1})	Mn (nmol Kg^{-1})	Y (nmol Kg^{-1})	Ca (mmol Kg^{-1})
Upriver	0.1	176.5	7.1	0.8	0.227
River mouth	11.1	273.7	217.2	1.1	1.049
Nearshore	35.8	174.8	8.5	0.2	0.908
Bay	36.1	72.3	9.1	0.2	1.116
Reef	35.5	71.5	8.8	0.2	1.067

[a] The concentrations of barium (Ba), manganese (Mn), yttrium (Y), and calcium (Ca) are given along with the salinity at each sampling site. All samples were collected on 19 March 2008.

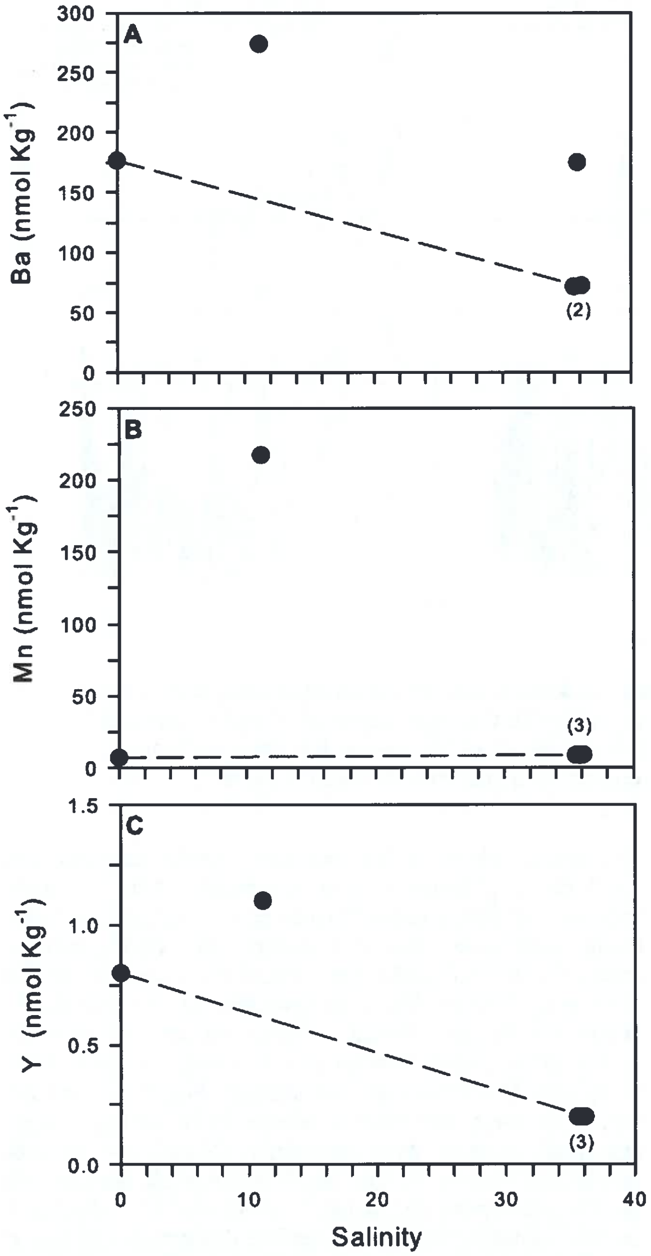

Figure 5. Concentrations of (a) barium, (b) manganese, and (c) yttrium along a salinity gradient from the Rio Fajardo to the coastal ocean. Theoretical conservative mixing is shown by the dashed lines. Numbers in parentheses indicate the number of discrete data points plotted where two or more data points overlap due to similar salinity values.

floodplains and estuaries can serve as storage reservoirs for Ba-rich sediments [*Edmond et al.*, 1978; *Li and Chan*, 1979; *Dorval et al.*, 2005]. Studies in both temperate and tropical coastal systems have identified both sporadic and gradual Ba desorption as being a key factor in controlling the concentration of dissolved Ba in coastal waters [*Carroll et al.*, 1993; *Coffey et al.*, 1997; *Dorval et al.*, 2005]. For example, sediments mobilized by one large discharge event may be stored in the estuary, and then gradual desorption by tidal mixing may produce a lag of increased coastal Ba concentration over several days, weeks, or longer. The observed lag between Ba/Ca and river discharge in the Fajardo coral was on the order of six weeks and therefore could be entirely explained by sporadic release of Ba from estuarine or floodplain-stored sediments.

[26] Additionally, Ba supply to rivers via physical and chemical weathering is typically limited in the tropics [*Edmond et al.*, 1978] and this limited Ba supply has been demonstrated using calibrated coral Ba/Ca records [*Sinclair and McCulloch*, 2004]. *Alibert et al.* [2003] proposed that increased precipitation and river volume could serve to dilute this limited supply of weathered Ba in tropical rivers. Under such conditions, coral Ba/Ca may be more reflective of cumulative, rather than instantaneous, river discharge and associated terrestrial Ba fluxes. Ba supply to tropical rivers can also be enhanced through increased soil respiration on land [*Markewitz et al.*, 2001]. Thus, increased Ba flux to the coastal ocean may not only be a product of increased river discharge, and this may account for the lags observed between river discharge and Ba/Ca in the Fajardo coral.

[27] The biology of the coral may also play a role in controlling the partitioning and apparent timing of minor and trace element incorporation into the skeleton. *Moyer and Grottoli* [2011] reported lower than normal growth rates in the Fajardo coral and other studies have shown links between terrigenous sediment inputs to the coastal ocean in Puerto Rico and reduced coral growth [*Loya*, 1976; *Morelock et al.*, 1983; *Torres and Morelock*, 2002]. *Pingitore et al.* [1989] have suggested that slow growth rates in *M. annularis* may lead to lower concentrations and less variability of skeletal Ba/Ca when compared to faster growing species. Slow growth by the coral has also been suggested as a possible mechanism to explain observed lags of other trace metals in high latitude [*Fallon et al.*, 1999] and eastern Pacific corals [*Matthews*, 2007]. Thus, the lower than average growth rate of the Fajardo coral [*Moyer and Grottoli*, 2011] could also explain the lag between river discharge and Ba/Ca peaks observed in the Fajardo coral.

4.2. Relationship Between Coral Ba/Ca, δ^{13}C, and Δ^{14}C

[28] Coral Ba/Ca increased as Rio Fajardo discharge increased and as coral skeletal δ^{13}C and Δ^{14}C both decreased (Figures 7 and 8). An inverse relationship between Ba and δ^{13}C was also reported in a Florida Bay coral that was thought to be influenced by freshwater input to the coastal ocean [*Swart et al.*, 1999]. Previous work by *Moyer and Grottoli* [2011] showed that coral skeletal δ^{13}C decreased as Rio Fajardo discharge increased and that both δ^{13}C and Δ^{14}C in the Fajardo coral reflected the delivery of δ^{13}C- and Δ^{14}C-depleted riverine DIC to the coastal ocean.

[29] Measurements of dissolved Ba from the river to the coastal ocean also support this interpretation (Table 1 and Figure 5a). Dissolved Ba exhibited clear desorptive behavior in the freshwater-seawater mixing zone (Figure 5a), and the surface water Ba concentration above the reef (71.5 nmol Kg^{-1}) was higher than open ocean values of 33–45 nmol Kg^{-1} reported by *Shen and Sanford* [1990] and *Alibert et al.* [2003]. However, since dissolved Ba was only measured in ambient water during one dry season, and this sampling occurred several years after the collection of the Fajardo coral, direct calibration of riverine, seawater, and coral Ba

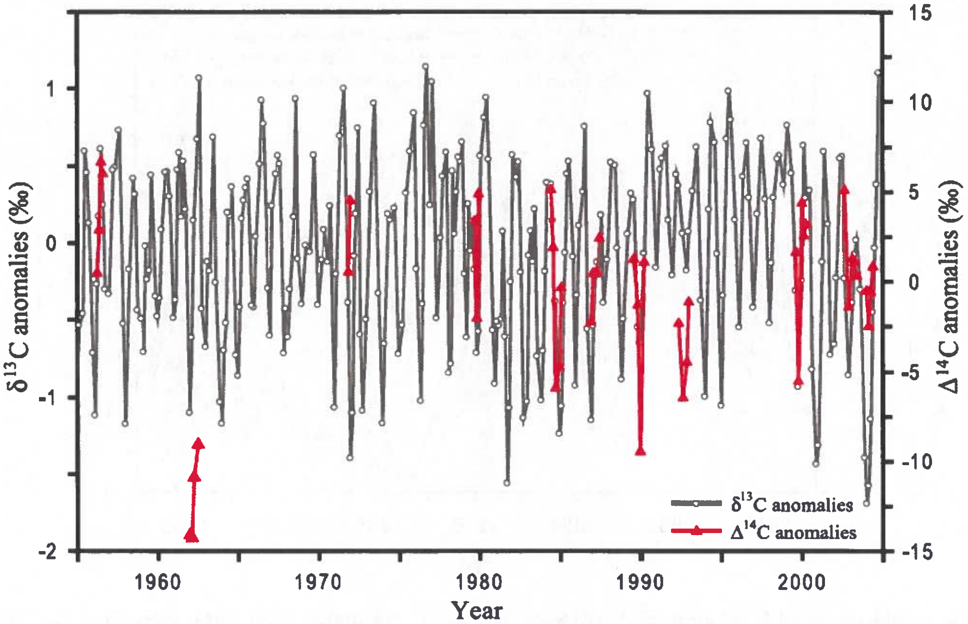

Figure 6. Stable ($\delta^{13}C$, circle) and radiocarbon ($\Delta^{14}C$, triangle) isotope anomalies in the Fajardo coral skeleton for the period 1955–2004. The $\delta^{13}C$ anomalies were generated by removing the trend of the ^{13}C Suess effect; $\Delta^{14}C$ anomalies were generated by removing the trend of the bomb radiocarbon curve. Data from *Moyer and Grottoli* [2011].

concentrations cannot be made at this time. Instead, Ba/Ca in the Fajardo coral can only provide an accurate record of the timing and duration of increased Rio Fajardo discharge to the coastal ocean over time.

4.3. Coral Mn/Ca and Y/Ca

[30] Manganese and yttrium in coral skeletons have also been implicated as markers of terrigenous input to the coastal ocean [*Alibert et al.*, 2003; *Wyndham et al.*, 2004; *Lewis et al.*, 2007, *Prouty et al.*, 2008; *Carilli et al.*, 2009; *Prouty et al.*, 2009]. However, coral Mn/Ca has been shown to be less reflective of river discharge and to have either no, or weak, correlation with coral Ba/Ca and/or river discharge [*Shen et al.*, 1992a; *Alibert et al.*, 2003; *Wyndham et al.*, 2004]. Additionally, coral Mn/Ca records have been shown to exhibit anomalously high, yet reproducible peaks which

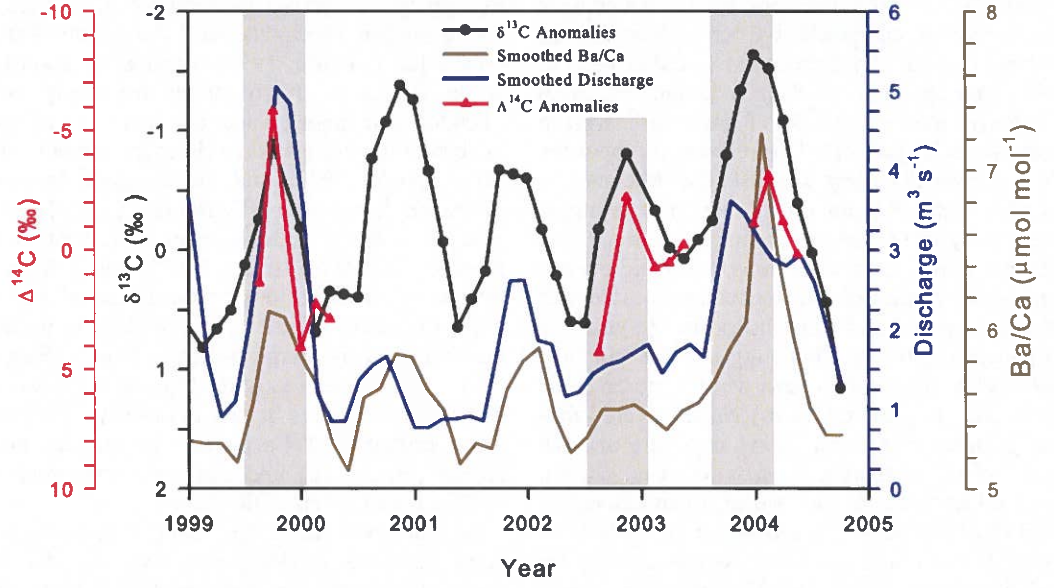

Figure 7. Fajardo coral $\delta^{13}C$ anomalies (black line), $\Delta^{14}C$ anomalies (red line), smoothed Ba/Ca (brown line), and Rio Fajardo discharge (blue line) from 1999 to 2004. Coral $\delta^{13}C$ and $\Delta^{14}C$ anomaly axes have been inverted to aid with visual interpretation. Gray vertical bars indicate the wet season for years where data for all three geochemical proxies and river discharge are present. Rio Fajardo discharge data obtained from USGS stream gauge station #50071000 (http://pr.water.usgs.gov).

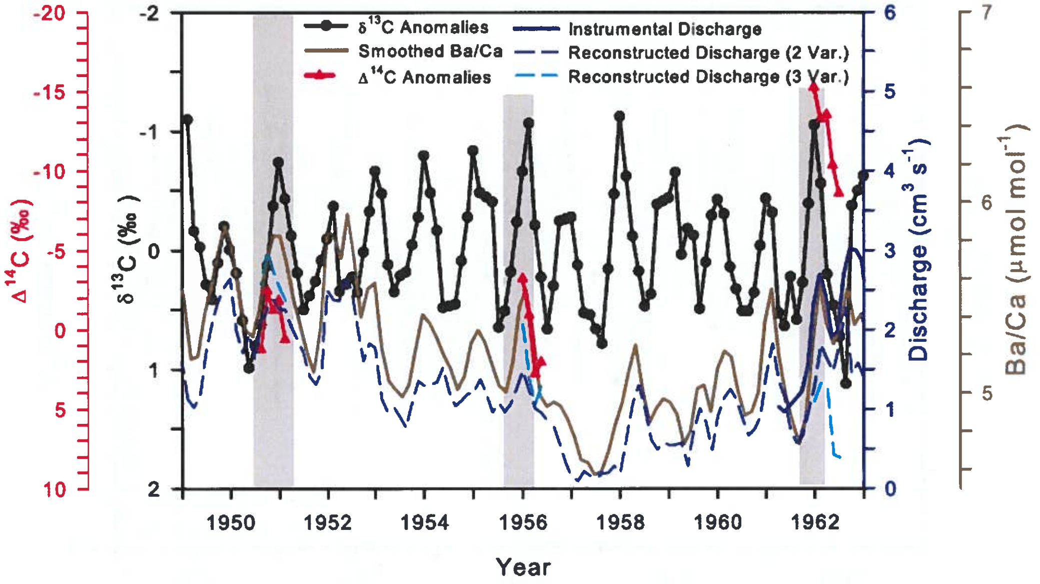

Figure 8. Fajardo coral δ^{13}C anomalies (black line), Δ^{14}C anomalies (red line), smoothed Ba/Ca (brown line), and reconstructed Rio Fajardo discharge (dashed dark blue line, two variables; dashed light blue line, three variables) from 1949 to 1963. Smoothed instrumental Rio Fajardo discharge is also shown (solid dark blue line). Coral δ^{13}C and Δ^{14}C anomaly axes have been inverted to aid with visual interpretation. Gray vertical bars indicate the approximate wet season during years where data for all three geochemical proxies are present. See section 4.4 of the text for details on discharge reconstruction.

do not correlate well with other minor and trace element records within the same coral or with river discharge [*Alibert et al.*, 2003]. Y/Ca has been shown to be correlated with (albeit with less sensitivity) seasonal and long-term changes in river discharge over time [e.g., *Alibert et al.*, 2003; *Lewis et al.*, 2007].

[31] Mn/Ca in the Fajardo coral (Figure 3c) was not coherent with river discharge on annual time scales (Figures 4e and 4f). Several anomalous Mn/Ca peaks were present within the record, and qualitative comparison showed that these did not consistently correspond to either peak or low-flow river discharge periods (Figures 3a and 3c). Coral Mn/Ca was however coherent with Rio Fajardo discharge on 2 and 4.5 year cycles (Figure 4f). This relationship between coral Mn/Ca and river discharge suggests that Mn may be associated with terrestrial input due to larger interannual tropical weather systems or climatic events. While the 2 year cyclicity does not correspond with known climatic events, the 4.5 year periodicity falls between the recurrence intervals of tropical storms (3 years) and minor hurricanes (6 years) in Puerto Rico [*Andrews*, 2007]. This suggests that Mn may only be mobilized to the coastal ocean when large episodic weather events (i.e., tropical cyclones) cause severe landscape erosion [*Scatena and Lugo*, 1995], exposure of fresh surfaces for chemical weathering [*Goldsmith et al.*, 2010], and changes in solute fluxes to the coastal ocean associated with increased river discharge [*Alexander et al.*, 2001].

[32] Although Mn in corals has been used as a proxy for terrestrial sediment input to the coastal ocean [e.g., *Lewis et al.*, 2007; *Prouty et al.*, 2008; *Carilli et al.*, 2009; *Prouty et al.*, 2009], the actual source of variability of Mn/Ca ratios in coral skeletons has remained elusive. Many studies have identified a range of possible sources of Mn to coral skeletons including volcanic activity [*Shen et al.*, 1991], resuspension of benthic sediments [*Shen et al.*, 1992b], and terrestrial nutrient and sediment fluxes [*Alibert et al.*, 2003; *Wyndham et al.*, 2004]. While Mn desorption from particulate material is known to occur in low-salinity waters in a manner similar to Ba (Figures 5a and 5b), the biogeochemical processes influencing Mn during and after desorption are much more complex [*Ouddane et al.*, 1997]. Although Mn is very sensitive to redox conditions common in tropical mangrove-lined estuaries, it does not form a stable sulfide precipitate as is common with other trace metals [*de Lacerda*, 1997]. Ecological studies suggest Mn is an important micronutrient for many marine phytoplankton and higher plants and has been measured in high concentration compared to other trace metals in mangroves [*de Lacerda*, 1997] and the common tropical sea grass *Thalassia testudinum* [*Whelan et al.*, 2005]. Dissolved Mn also has a strong preference for adsorption onto carbonate particles [*Ouddane et al.*, 1997]. These factors may combine to explain the low concentration of Mn measured in coastal seawater (Table 1) and the lack of annual coherence between river discharge and coral Mn/Ca (Figure 4f).

[33] Y/Ca measured in the Fajardo coral was not coherent with river discharge at any periodicity. Additionally, transient anomalous Y/Ca peaks were present throughout the record (Figure 3d) and did not correspond with similar Mn/Ca peaks or river discharge.

[34] *Alibert et al.* [2003] found Y to be more enriched in coral skeletons growing near river mouths, however the coral Y/Ca record was less sensitive to river discharge than Ba/Ca on annual time scales. Average Y/Ca over the entire Fajardo coral record was 0.03 ± 0.02 μmol mol^{-1}, which is larger than the average reported by *Alibert et al.* [2003] for an offshore coral not influenced by a river plume. Dissolved Y also exhibited nonconservative mixing, with a source of

Table 2. The Statistical Relationships Between Coral Geochemical Data and River Discharge as Determined by Multiple-Regression Analysis[a]

Variable	Coefficient	Error[b]	P
	Two-Variable Model[c]		
Ba/Ca	2.077	0.501	<0.001
$\delta^{13}C$	0.329	0.266	0.223
Intercept	−9.601	2.763	0.001
	Three-Variable Model[d]		
Ba/Ca	1.854	0.964	0.083
$\delta^{13}C$	0.693	0.822	0.419
$\Delta^{14}C$	−0.127	0.131	0.354
Intercept	−7.969	5.350	0.167

[a] Data are presented for a two-variable (coral Ba/Ca and δ13C) and three-variable (coral Ba/Ca, $\delta^{13}C$, and $\Delta^{14}C$) model.

[b] Reported error is one standard error of the mean (±1 SEM).

[c] $R = 0.634$, $R^2 = 0.402$, $R^2_{Adj} = 0.3737$; Discharge = (Ba/Ca × 2.077) + ($\delta^{13}C$ × 0.329) − 9.601.

[d] $R = 0.673$, $R^2 = 0.452$, $R^2_{Adj} = 0.288$; Discharge = (Ba/Ca × 1.854) + ($\delta^{13}C$ × 0.693) − ($\Delta^{14}C$ × 0.127) − 9.601.

Y in the low-salinity waters (Figure 5c), similar to the desorptive behavior of Ba and Mn. Although this creates the potential for Y/Ca ratios in the Fajardo coral to reflect Rio Fajardo discharge, the two time series were not coherent nor did large Y/Ca peaks reflect times of increased river discharge (Figure 3). Although *Lewis et al.* [2007] were able to infer historical terrestrial sediment fluxes from interannual coral records of Y, the annual variability of Y/Ca in corals does not appear to accurately reflect annual patterns in river discharge in the Fajardo coral.

4.4. Implications for Proxy Records

[35] Given the strong coherence of Ba/Ca and $\delta^{13}C$ in the coral record (Figure 4d) and the coherence of each of those geochemical records with river discharge (Figure 4b) [*Moyer and Grottoli*, 2011], the combined use of Ba/Ca and carbon isotopes (both $\delta^{13}C$ and $\Delta^{14}C$) can provide a clear history of terrestrial river discharge, and carbon and elemental fluxes from land to the coastal ocean. Such records may be extremely useful in areas where rivers are not gauged, and the delivery of terrestrial material the coastal ocean is poorly quantified. For example, Figure 7 shows coral skeletal $\delta^{13}C$, $\Delta^{14}C$, and Ba/Ca for the most recent 5 years of the Fajardo coral record (1999–2004), which overlaps with available records of Rio Fajardo discharge. For years where all three coral proxies are available (1999, 2002, 2003/2004; Figure 7), there is very good agreement between the timing of increased river discharge, increased Ba/Ca and decreases in $\delta^{13}C$ and $\Delta^{14}C$. The increases in coral Ba/Ca clearly coincide with the timing of increased Rio Fajardo discharge during the wet season as discussed above. In addition, the depletions of $\delta^{13}C$ and $\Delta^{14}C$ which also are influenced by river discharge (see discussion by *Moyer and Grottoli* [2011]) are nearly synchronous with the increases in Ba/Ca (Figure 7).

[36] Because the three proxies can all be linked to freshwater discharge and occur consistently with the same timing in the coral record, this strongly suggests that the Fajardo coral is recording the delivery of freshwater and terrestrial material to the coastal ocean. Thus, these relationships were statistically modeled using multiple-regression analysis in the portion of the record where instrumental discharge and coral geochemical data ($\delta^{13}C$, $\Delta^{14}C$, and Ba/Ca) were available (1963–2004) in an attempt to reconstruct discharge for a portion of the coral geochemical record where instrumental discharge was not available (194–1962; Table 2 and Figure 8). The reconstructed discharge shows good temporal agreement between the instrumental record, and the timing of increases in coral Ba/Ca and depletions of coral $\delta^{13}C$ and $\Delta^{14}C$ (Figure 8). From these records it is then possible to infer the approximate timing of the wet season in each of those years where instrumental records are not available (Figure 8). While the timing of increases in reconstructed discharge corresponded well with the instrumental record and known timing of the wet season in Puerto Rico, the magnitude of the reconstructed discharge is consistently less than that of the instrumental discharge when only two variables Ba/Ca and $\delta^{13}C$) are used to reconstruct discharge (Figure 8). The inclusion of all three variables (Ba/Ca, $\delta^{13}C$ and $\Delta^{14}C$) produced a reconstructed discharge values with larger amplitude in 1951 and 1955. Thus, a three-proxy model may yield discharge reconstructions which reflect actual discharge values. Additionally, it is also necessary to measure $\Delta^{14}C$ since coral skeletal $\delta^{13}C$ can also be influenced by metabolic processes of the coral animal (see discussion by *Moyer and Grottoli* [2011]). The three-proxy-reconstructed discharge in 1961–1962 had values that were lower than both the instrumental discharge and the two-variable discharge reconstruction (Figure 8). However, these reconstructed discharge values are likely spurious due to the large negative $\Delta^{14}C$ anomalies caused by the introduction of bomb radiocarbon into the coral record in 1961–1962 (see discussions by *Grottoli and Mark Eakin* [2007] and *Moyer and Grottoli* [2011]). Thus, care should be taken when interpreting discharge reconstructions during the decade of peak bomb-radiocarbon increase in natural $\Delta^{14}C$ records (1961 – 1973).

[37] Since the Ba/Ca, $\delta^{13}C$ and $\Delta^{14}C$ of corals growing near the mouths of SMRs are influenced by riverine discharge and the same coral skeletal $\delta^{13}C$ and $\Delta^{14}C$ are influenced by the isotopic composition of the riverine DIC [*Moyer and Grottoli*, 2011], it should also be possible to use $\delta^{13}C$, $\Delta^{14}C$, and Ba/Ca from these types of corals to reconstruct local terrestrial material fluxes from SMRs to the coastal ocean. Sediment yields, for instance, could be determined using reconstructed discharge values and constructing sediment rating curves for a given SMR [*Asselman*, 2000]. Since many tropical corals have long lifespans, such a multiproxy approach could also yield records of tropical land ocean carbon and elemental fluxes spanning several centuries for many areas where discharge data from SMRs are few, and local material fluxes to the coastal ocean are not well understood. This is of particular importance for tropical areas like Puerto Rico where there have been major land use changes to or from natural vegetation (C_3 plants) to C_4-plant-dominated agricultural crops, leading to changes in coastal runoff and sedimentation.

[38] However the multiple-proxy technique for constructing river discharge described here is not without its current limitations and further study is required to understand the quantitative relationships between precipitation, discharge, and coral geochemistry. The nature of river discharge in the Fajardo catchment is such that while increases in

precipitation generally correspond to increases in river discharge, the intensity of the discharge event is not always proportional to the amount of precipitation (Figure 3a) [*Kilbourne et al.*, 2011]. Similarly, while large peaks in coral Ba/Ca, and decreases in δ^{13}C and Δ^{14}C generally correspond to increases in river discharge, the peaks are not always proportional to the size of the discharge event (Figures 3a and 3b), leading to a mismatch between intensities between instrumental and reconstructed discharge (Figure 8). We hypothesize that the largest discharge events create conditions detrimental to the growth of the coral, thus limiting the fidelity of geochemical preservation of the discharge signal during the largest events. While this and a study by *Moyer and Grottoli* [2011] provide the foundation and rational for such a multiproxy approach to reconstructing SMR discharge, additional experimental studies in controlled environments (i.e., tank experiments) are necessary in order to make this multiproxy approach a fully quantitative record of the flux of terrestrially derived carbon and other solutes to the coastal ocean.

5. Summary

[39] In this study, the minor and trace elements Ba, Ca, and Y (Figure 3) were measured in combination with paired measurements of δ^{13}C and Δ^{14}C (Figure 6) in the skeleton of a coral growing near the mouth of an SMR in eastern Puerto Rico (Figure 1). Coral Ba/Ca was highly coherent with both annual river discharge and coral skeletal δ^{13}C (Figures 4b and 4d), and increases in coral Ba/Ca were synchronous with the timing of depletions of both δ^{13}C and Δ^{14}C in the coral skeleton (Figures 7 and 8) and increases in river discharge (Figure 7). The strong coherence between the SMR discharge and Ba/Ca, and the concurrent timing of increases in Ba/Ca with decreases in δ^{13}C and Δ^{14}C support hypotheses 1 and 2 (see section 1) and demonstrate that the Fajardo coral is recording the influence of riverine waters in the coastal ocean. Furthermore, the synchronous timing of Ba/Ca increases with depletions of coral skeletal δ^{13}C and Δ^{14}C were coincident with the known wet season in eastern Puerto Rico. These data support hypotheses 2 and 3 (see section 1) and demonstrate that SMR discharge is recorded by multiple geochemical records, which can also be used as proxies of terrestrial material flux to the coastal ocean. Of the three minor and trace element records examined, coral Ba/Ca was the only one to be annually coherent with river discharge. Although Mn/Ca and Y/Ca were also expected to record river discharge, the data from the Fajardo coral did not support this hypothesis and suggest that Mn/Ca and Y/Ca in coral skeletons are not good proxies of annual river discharge. However, the data show that coral skeletal records of Ba/Ca, δ^{13}C and Δ^{14}C are all indicative of river discharge to the coastal ocean, and thus can provide a means to reconstruct river discharge to the coastal ocean in the tropics. With additional experimental calibration, this combination of Ba/Ca and carbon isotopes in coral skeletons could be developed to provide a robust quantitative proxy for the history of terrigenous material and carbon flux to the coastal ocean over the last several centuries for many tropical SMRs where historical and instrumental records are scarce.

[40] **Acknowledgments.** This work was supported primarily by grants to A.G.G. from the Andrew W. Mellon Foundation and the National Science Foundation (OCE-0610487). Funding for the LA-ICP-SFMS equipment was provided by the Ohio Board of Regents Hayes Investment Fund. R.P.M. was a graduate student in A.G.G.'s lab during the execution of this work and was partially supported by an OSU Presidential Fellowship and grants from the American Association of Petroleum Geologists, the American Geophysical Union, the Geological Society of America, and the Friends of Orton Hall. R.P.M. was supported by a USGS Mendenhall Postdoctoral Fellowship during the preparation of the manuscript. We are grateful for field assistance provided by H. Anguerre, M. Canals, M. Cathey, C. Malachowski, C. Pacheco, and B. Williams. K. Helmle and R. Dodge facilitated the X-radiography of the coral skeletons at the National Coral Reef Institute. Lab analyses were assisted by M. Cathey, A. Lutton, Y. Matsui, C. Paver, L. Swierk, and H. Wu. We thank G. dos Santos and J. Southon (Keck AMS) for assistance with ^{14}C analyses and data processing. We are grateful to J. Bauer, A. Carey, Y-P. Chin, D. Lea, M. Saltzman, A. Shinohara, B. Williams, and three anonymous persons for their careful reviews and suggestions, which improved the overall quality of the manuscript.

References

Alexander, J., C. R. Fielding, S. J. Wakefield, M. T. George, and C. F. Cottnam (2001), Fluvial geochemistry through a short-duration, tropical-cyclone induced discharge event in the Burdekin River and Hann Creek, North Queensland, Australia, *Aquat. Geochem.*, *7*, 275–293, doi:10.1023/A:1015203127320.

Alibert, C., L. Kinsley, S. J. Fallon, M. T. McCulloch, R. Berkelmans, and F. McAllister (2003), Source of trace element variability in Great Barrier Reef corals affected by the Burdekin flood plumes, *Geochim. Cosmochim. Acta*, *67*, 231–246, doi:10.1016/S0016-7037(02)01055-4.

Andrews, A. J. (2007), Spatial and temporal variability of tropical storm and hurricane strikes in the Bahamas, and the Greater and Lesser Antilles, MS thesis, 79 pp., La. State Univ., Baton Rouge.

Asselman, N. E. M. (2000), Fitting and interpretation of sediment rating curves, *J. Hydrol.*, *234*, 228–248, doi:10.1016/S0022-1694(00)00253-5.

Buddemeier, R. W., and R. A. Kinzie (1976), Coral growth, *Oceanogr. Mar. Biol.*, *14*, 183–225.

Carilli, J. E., N. G. Prouty, K. A. Hughen, and R. D. Norris (2009), Century-scale records of land-based activities recorded in Mesoamerican coral cores, *Mar. Pollut. Bull.*, *58*, 1835–1842, doi:10.1016/j.marpolbul.2009.07.024.

Carroll, J., K. K. Falkner, E. T. Brown, and W. S. Moore (1993), The role of the Ganges-Brahmaputra mixing zone in supplying barium and ^{226}Ra to the Bay of Bengal, *Geochim. Cosmochim. Acta*, *57*, 2981–2990, doi:10.1016/0016-7037(93)90287-7.

Chatfield, C. (2004), *The Analysis of Time Series: An Introduction*, 6th ed., 333 pp., Chapman and Hall, Boca Raton, Fla.

Clark, J. J., and P. R. Wilcock (2000), Effects of land-use change on channel morphology in northeastern Puerto Rico, *Geol. Soc. Am. Bull.*, *112*, 1763–1777, doi:10.1130/0016-7606(2000)112<1763:EOLUCO>2.0.CO;2.

Coffey, M., F. Dehairs, O. Collette, G. Luther, T. Church, and T. Jickells (1997), The behaviour of dissolved barium in estuaries, *Estuarine Coastal Shelf Sci.*, *45*, 113–121, doi:10.1006/ecss.1996.0157.

Coplen, T. B. (1996), New guidelines for reporting stable hydrogen, carbon, and oxygen isotope-ratio data, *Geochim. Cosmochim. Acta*, *60*, 3359–3360, doi:10.1016/0016-7037(96)00263-3.

Craig, C.-A., K. E. Jarvis, and L. J. Clarke (2000), An assessment of calibration strategies for the quantitative and semi-quantitative analysis of calcium carbonate matrices by laser ablation-inductively coupled plasma-mass spectrometry (LA-ICP-MS), *J. Anal. At. Spectrom.*, *15*, 1001–1008, doi:10.1039/b002097o.

de Lacerda, L. D. (1997), Trace metals in mangrove plants: Why such low concentrations?, in *Mangrove Ecological Studies in Latin America and Africa*, edited by B. Kjerfve, L. D. de Lacerda, and E. S. Diop, pp. 71–78, U. N. Educ. Sci. Cult. Organ., Paris.

Dorval, E., C. M. Jones, and R. Hannigan (2005), Chemistry of surface waters: Distinguishing fine-scale differences in sea grass habitats of Chesapeake Bay, *Limnol. Oceanogr.*, *50*, 1073–1083, doi:10.4319/lo.2005.50.4.1073.

Druffel, E. R. M. (1997), Geochemistry of corals: Proxies of past ocean chemistry, ocean circulation, and climate, *Proc. Natl. Acad. Sci. U. S. A.*, *94*, 8354–8361, doi:10.1073/pnas.94.16.8354.

Edmond, J. M., E. D. Boyle, D. Drummond, B. Grant, and T. Mislick (1978), Desorption of barium in the plume of the Zaire (Congo) River, *Neth. J. Sea Res.*, *12*, 324–328, doi:10.1016/0077-7579(78)90034-0.

Esslemont, G., R. A. Russell, and W. A. Maher (2004), Coral record of harbour dredging: Townsville, Australia, *J. Mar. Syst.*, *52*, 51–64, doi:10.1016/j.jmarsys.2004.01.005.

Fallon, S. J., M. T. McCulloch, R. van Woesik, and D. J. Sinclair (1999), Corals at their latitudinal limits: Laser ablation trace element systematics in *Porites* from Shirigai Bay, Japan, *Earth Planet. Sci. Lett.*, *172*, 221–238, doi:10.1016/S0012-821X(99)00200-9.

Fallon, S. J., J. C. White, and M. T. McCulloch (2002), *Porites* corals as recorders of mining and environmental impacts: Misima Island, Papua New Guinea, *Geochim. Cosmochim. Acta*, *66*, 45–62, doi:10.1016/S0016-7037(01)00715-3.

Fleitmann, D., R. B. Dunbar, M. McCulloch, M. Mudelsee, M. Vuille, T. R. McClanahan, J. E. Cole, and S. Eggins (2007), East African soil erosion recorded in a 300 year old coral colony from Kenya, *Geophys. Res. Lett.*, *34*, L04401, doi:10.1029/2006GL028525.

Gagan, M. K., L. K. Ayliffe, J. W. Beck, J. E. Cole, E. R. M. Druffel, R. B. Dunbar, and D. P. Schrag (2000), New views of tropical paleoclimates from corals, *Quat. Sci. Rev.*, *19*, 45–64, doi:10.1016/S0277-3791(99)00054-2.

Gellis, A. (2003), Suspended-sediment characteristics in four humid tropical watersheds of contrasting land use, Puerto Rico, PhD thesis, 697 pp., Dep. of Earth Resour., Colo. State Univ., Fort Collins.

Goenaga, C., and G. Cintron (1979), Inventory of the Puerto Rican coral reefs, 193 pp., Dep. of Nat. Resour., San Juan, Puerto Rico.

Goldsmith, S. T., A. E. Carey, B. M. Johnson, S. A. Welch, W. B. Lyons, W. H. McDowell, and J. S. Pigott (2010), Stream geochemistry, chemical weathering and CO_2 consumption potential of andesitic terrains, Dominica, Lesser Antilles, *Geochim. Cosmochim. Acta*, *74*, 85–103, doi:10.1016/j.gca.2009.10.009.

Grau, H. R., T. M. Aide, J. K. Zimmerman, J. R. Thomlinson, E. Helmer, and X. Zou (2003), The ecological consequences of socioeconomic and land-use changes in postagriculture Puerto Rico, *BioScience*, *53*, 1159–1168.

Grottoli, A. G., and C. Mark Eakin (2007), A review of modern coral $\delta^{18}O$ and $\Delta^{14}C$ proxy records, *Earth Sci. Rev.*, *81*, 67–91, doi:10.1016/j.earscirev.2006.10.001.

Hart, S. R., and A. L. Cohen (1996), An ion probe study of annual cycles of Sr/Ca and other trace elements in corals, *Geochim. Cosmochim. Acta*, *60*, 3075–3084, doi:10.1016/0016-7037(96)00154-8.

Hearn, P., et al. (2001), *Global GIS Database: Digital Atlas of Central and South America* [CD-ROM], U.S. Geol. Surv., Washington, D. C.

Kilbourne, K. H., R. P. Moyer, T. M. Quinn, and A. G. Grottoli (2011), Testing coral-based tropical cyclone reconstructions: An example from Puerto Rico, *Palaeogeogr. Palaeoclimatol. Palaeoecol.*, *307*, 90–97, doi:10.1016/j.palaeo.2011.04.027.

Knutson, D. W., R. W. Buddemeier, and S. V. Smith (1972), Coral chronometers: Seasonal growth bands in reef corals, *Science*, *177*, 270–272, doi:10.1126/science.177.4045.270.

Lea, D. W., G. T. Shen, and E. A. Boyle (1989), Coralline barium records temporal variability in equatorial Pacific upwelling, *Nature*, *340*, 373–376, doi:10.1038/340373a0.

Lewis, S. E., G. A. Shields, B. S. Kamber, and J. M. Lough (2007), A multi-trace element coral record of land-use changes in the Burdekin River catchment, NE Australia, *Palaeogeogr. Palaeoclimatol. Palaeoecol.*, *246*, 471–487, doi:10.1016/j.palaeo.2006.10.021.

Li, Y.-H., and L.-H. Chan (1979), Desorption of Ba and ^{226}Ra from river-borne sediments in the Hudson estuary, *Earth Planet. Sci. Lett.*, *43*, 343–350, doi:10.1016/0012-821X(79)90089-X.

López, T. M., T. M. Aide, and J. R. Thomlinson (2001), Urban expansion and the loss of prime agricultural lands in Puerto Rico, *Ambio*, *30*, 49–54.

Loya, Y. (1976), Effects of water turbidity and sedimentation on the community structure of Puerto Rican corals, *Bull. Mar. Sci.*, *26*, 450–466.

Lugo, A. E., and E. Helmer (2004), Emerging forests on abandoned land: Puerto Rico's new forests, *For. Ecol. Manage.*, *190*, 145–161.

Lyons, W. B., C. A. Nezat, A. E. Carey, and D. M. Hicks (2002), Organic carbon fluxes to the ocean from high-standing islands, *Geology*, *30*, 443–446, doi:10.1130/0091-7613(2002)030<0443:OCFTTO>2.0.CO;2.

Mark Eakin, C., and A. G. Grottoli (2006), Coral reef records of past climatic change, in *Coral Reefs and Climate Change: Science and Management*, *Coastal Estuarine Stud.*, vol. 61, edited by J. T. Phinney et al., pp. 33–54, AGU, Washington, D. C., doi:10.1029/61CE04.

Markewitz, D., E. A. Davidson, R. O. Figueiredo, R. L. Victoria, and A. V. Krusche (2001), Control of cation concentrations in stream waters by surface soil processes in an Amazonian watershed, *Nature*, *410*, 802–805, doi:10.1038/35071052.

Matthews, K. A. (2007), Cadmium in coral skeleton: Natural variability and in situ calibration, PhD dissertation, Univ. of Penn., Philadelphia.

McCulloch, M., S. Fallon, T. Wyndham, E. Hendy, J. Lough, and D. Barnes (2003), Coral record of increased sediment flux to the inner Great Barrier Reef since European settlement, *Nature*, *421*, 727–730, doi:10.1038/nature01361.

Milliman, J. D., and J. P. M. Syvitski (1992), Geomorphic/tectonic control of sediment discharge to the ocean: The importance of small mountainous rivers, *J. Geol.*, *100*, 525–544, doi:10.1086/629606.

Morelock, J., K. Grove, and M. L. Hernandez (1983), Oceanography and patterns of shelf sediments, Mayaguez, Puerto Rico, *J. Sediment. Res.*, *53*, 371–381.

Moyer, R. P., and A. G. Grottoli (2011), Coral skeletal carbon isotopes ($\delta^{13}C$ and $\Delta^{14}C$) record the delivery of terrestrial carbon to the coastal waters of Puerto Rico, *Coral Reefs*, *30*, 791–802, doi:10.1007/s00338-011-0758-y.

Ouddane, B., E. Martin, A. Boughriet, J. C. Fischer, and M. Wartel (1997), Speciation of dissolved and particulate manganese in the Seine river estuary, *Mar. Chem.*, *58*, 189–201, doi:10.1016/S0304-4203(97)00034-0.

Pearce, N. J. G., W. T. Perkins, J. A. Westgate, M. P. Gorton, S. E. Jackson, C. R. Neal, and S. P. Chenery (1997), A compilation of new and published major and trace element data for NIST SRM 610 and NIST SRM 612 glass reference materials, *Geostand. Newsl.*, *21*, 115–144, doi:10.1111/j.1751-908X.1997.tb00538.x.

Pingitore, N. E., Y. Rangel, and A. Kwarteng (1989), Barium variation in *Acropora palmata* and *Montastrea annularis*, *Coral Reefs*, *8*, 31–36, doi:10.1007/BF00304689.

Prouty, N. G., K. A. Hughen, and J. Carilli (2008), Geochemical signature of land-based activities in Caribbean coral surface samples, *Coral Reefs*, *27*, 727–742, doi:10.1007/s00338-008-0413-4.

Prouty, N. G., S. D. Jupiter, M. E. Field, and M. T. McCulloch (2009), Coral proxy record of decadal-scale reduction in base flow from Moloka'i, Hawaii, *Geochem. Geophys. Geosyst.*, *10*, Q12018, doi:10.1029/2009GC002714.

Prouty, N. G., M. E. Field, J. D. Stock, S. D. Jupiter, and M. McCulloch (2010), Coral Ba/Ca records of sediment input to the fringing reef of the southshore of Moloka'i, Hawai'i over the last several decades, *Mar. Pollut. Bull.*, *60*, 1822–1835, doi:10.1016/j.marpolbul.2010.05.024.

Scatena, F. N., and A. E. Lugo (1995), Geomorphology, disturbance, and the soil and vegetation of two subtropical wet steepland watersheds of Puerto Rico, *Geomorphology*, *13*, 199–213, doi:10.1016/0169-555X(95)00021-V.

Shen, G. T., and C. L. Sanford (1990), Trace element indicators of climate change in annually banded corals, in *Global Consequences of the 1982–83 El Nino-Southern Oscillation*, edited by P. W. Glynn, *Elsevier Oceanogr. Ser.*, *52*, 255–283.

Shen, G. T., T. M. Campbell, R. B. Dunbar, G. M. Wellington, M. W. Colgan, and P. W. Glynn (1991), Paleochemistry of manganese in corals from the Galapagos Islands, *Coral Reefs*, *10*, 91–100, doi:10.1007/BF00571827.

Shen, G. T., J. E. Cole, D. W. Lea, L. J. Linn, T. A. McConnaughey, and R. G. Fairbanks (1992a), Surface ocean variability at Galapagos from 1936–1982: Calibration of geochemical tracers in corals, *Paleoceanography*, *7*, 563–588, doi:10.1029/92PA01825.

Shen, G. T., L. J. Linn, T. M. Campbell, J. E. Cole, and R. G. Fairbanks (1992b), A chemical indicator of trade wind reversal in corals from the western tropical Pacific, *J. Geophys. Res.*, *97*, 12,689–12,697, doi:10.1029/92JC00951.

Sinclair, D. J. (2005), Non-river flood barium signals in the skeletons of corals from coastal Queensland, Australia, *Earth Planet. Sci. Lett.*, *237*, 354–369, doi:10.1016/j.epsl.2005.06.039.

Sinclair, D. J., and M. T. McCulloch (2004), Corals record low mobile barium concentrations in the Burdekin River during the 1974 flood: Evidence for limited Ba supply to rivers?, *Palaeogeogr. Palaeoclimatol. Palaeoecol.*, *214*, 155–174.

Sinclair, D. J., L. P. J. Kinsley, and M. T. McCulloch (1998), High resolution analysis of trace elements in corals by laser ablation ICP-MS, *Geochim. Cosmochim. Acta*, *62*, 1889–1901, doi:10.1016/S0016-7037(98)00112-4.

Stuiver, M., and H. A. Polach (1977), Discussion: Reporting of ^{14}C data, *Radiocarbon*, *19*, 355–363.

Swart, P. K., G. Healy, L. Greer, M. Lutz, A. Saied, D. Anderegg, R. E. Dodge, and D. Rudnick (1999), The use of proxy chemical records in coral skeletons to ascertain past environmental conditions in Florida Bay, *Estuaries Coasts*, *22*, 384–397, doi:10.2307/1353206.

Thomas, R. (2003), *Practical Guide to ICP-MS*, 336 pp., Marcel Dekker, New York.

Thompson, R. O. R. Y. (1979), Coherence significance levels, *J. Atmos. Sci.*, *36*, 2020–2021, doi:10.1175/1520-0469(1979)036<2020:CSL>2.0.CO;2.

Torres, J. L., and J. Morelock (2002), Effect of terrigenous sediment influx on coral cover and linear extension rates of three Caribbean massive coral species, *Caribb. J. Sci.*, *38*, 222–229.

Tudhope, A. W., D. W. Lea, G. B. Shimmield, C. B. Chilcott, and S. Head (1996), Monsoon climate and Arabian Sea coastal upwelling recorded in massive corals from southern Oman, *Palaios*, *11*, 347–361, doi:10.2307/3515245.

Weldeab, S., D. W. Lea, R. R. Schneider, and N. Anderson (2007a), Centennial scale climate instabilities in a wet early Holocene West African monsoon, *Geophys. Res. Lett.*, *34*, L24702, doi:10.1029/2007GL031898.

Weldeab, S., D. W. Lea, R. R. Schneider, and N. Anderson (2007b), 155,000 years of West African monsoon and ocean thermal evolution, *Science*, *316*, 1303–1307, doi:10.1126/science.1140461.

Whelan, T., III, J. Espinoza, X. Villarreal, and M. CottaGoma (2005), Trace metal partitioning in *Thalassia testudinum* and sediments in the Lower Laguna Madre, Texas, *Environ. Int.*, *31*, 15–24, doi:10.1016/j.envint.2004.05.010.

Wyndham, T., M. McCulloch, S. Fallon, and C. Alibert (2004), High-resolution coral records of rare earth elements in coastal seawater: Biogeochemical cycling and a new environmental proxy, *Geochim. Cosmochim. Acta*, *68*, 2067–2080, doi:10.1016/j.gca.2003.11.004.